PII: S0032-3861(96)00715-X

Polymer Vol. 38 No. 8, pp. 1835–1843, 1997

0032-3861/97/$17.00 + 0.00

Toughening of cyanate ester resins with cyanated polysulfones

J. W. Hwang, S. D. Park, K. Cho, J. K. Kim and C. E. Park*
Department of Chemical Engineering, Pohang University of Science and Technology, San 31 Hyoja Dong, Pohang 790-784, Korea

and T. S. Oh
Polymeric Materials Division, Research Institute of Industrial Science and Technology, San 32 Hyoja Dong, Pohang 790-600, Korea
(Received 1 April 1996; revised 13 June 1996)

Bisphenol-A dicyanate (BADCy) resin was toughened by incorporating polysulfone (PSF) and cyanated polysulfone (CN-PSF). CN-PSF was synthesized by the bromination of PSF and cyanation. The effects of PSF content and interfacial adhesion between the matrix and the domain were investigated on the fracture toughness and morphology of BADCy/PSF blends. PSF formed a matrix phase when more than 20 parts per hundred of resin (phr) of PSF was incorporated. The particle size of BADCy decreased with increasing numbers of cyano groups in PSF. There was an optimum cyano group content for maximizing the fracture toughness of BADCy/CN-PSF blends with 30 phr of CN-PSF content. Toughening mechanisms were examined using scanning electron microscopy and transmission optical microscopy.

(Keywords: bisphenol-A dicyanate; cyanated polysulfone; fracture toughness)

INTRODUCTION

Cyanate ester resins are currently important thermosetting materials for the encapsulation of electronic devices, high-temperature adhesives and structural aerospace materials since they have excellent mechanical, thermal and adhesive properties[1–8]. The cyanate ester monomers undergo polycyclotrimerization to form highly cross-linked polycyanurates[6–8]. However, their inherent brittleness is a major drawback. To try and toughen the highly cross-linked thermosets, many researchers used rubber toughening, but without success because yielding of thermosetting matrices cannot be induced owing to the highly cross-linked structures[9–12]. Therefore, as an alternative to rubber toughening, toughening of highly cross-linked thermosets was achieved by physical blending with high-performance engineering thermoplastics such as poly(ether imide) (PEI)[13–15], poly(ether sulfone) (PES)[16,17] and poly(ether ketone) (PEK)[18]. Although thermosetting resins such as epoxies and bismaleimides were significantly toughened by incorporating non-reactive thermoplastic modifiers, the chemical resistance of thermoplastic modified thermosets was not acceptable. However, it has been recently reported that reactive functional groups such as hydroxyl and amino groups can be introduced into commercial thermoplastic modifiers to enhance the chemical resistance[19–21]. Many studies have also shown that the morphology and mechanical properties of thermoplastic modified thermosets are altered by introducing reactive functional groups into the thermoplastic modifiers[22–24].

In this study, cyanated polysulfones (PSFs) were synthesized as toughening agents for cyanate ester resins. The mechanical properties and morphology of PSF-modified cyanate ester resins were investigated by varying the PSF and cyano group content in the PSF.

EXPERIMENTAL

Materials

Bisphenol-A dicyanate (BADCy) manufactured by Rhone Poulenc was used as received without further purification. PSF (Rhone Poulenc's Udel P-3500) was used as a toughening agent. *Figure 1* shows the chemical structures of BADCy and PSF.

Modification of PSF

Functional groups were introduced into PSF via two-step reactions:

Bromination	$\text{PSF-H} + \text{Br}_2 \rightarrow \text{Br-PSF} + \text{HBr}$
Cyanation	$\text{Br-PSF} + \text{CuCN} \rightarrow \text{CN-PSF} + \text{CuBr}$

Bromination of PSF

Hydrogens in the phenyl rings of PSF were substituted by bromine via a nucleophilic aromatic substitution reaction at room temperature. PSF (50 g) was dissolved in methylene chloride (600 ml) in a two-necked round-bottomed flask equipped with a condenser, and then iodine dissolved in 50 ml of methylene chloride was added to the PSF solution. The number of bromine atoms per PSF chain was controlled by varying the

* To whom correspondence should be addressed

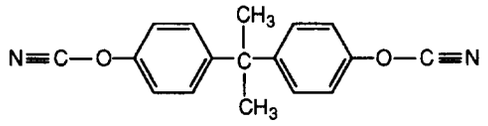

Bisphenol-A dicyanate (BADCy)

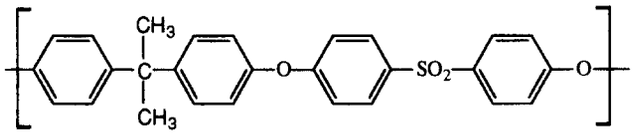

Polysulfone (PSF)

Figure 1 Chemical structures of BADCy and PSF

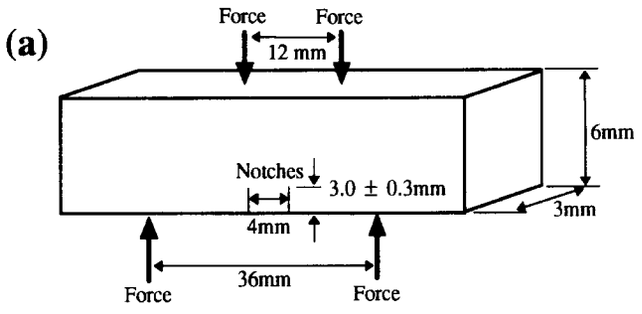

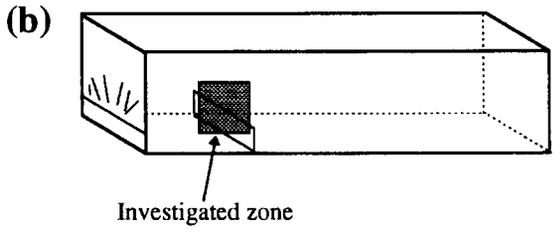

Figure 2 Schematic diagrams of (a) the DN-4PB geometry and (b) the region from the DN-4PB specimen for optical microscope investigations

amount of iodine catalyst. After mixing the solution with a magnetic stirring bar, 10 ml of bromine dissolved in 40 ml of methylene chloride was slowly added using a dropping funnel over 30 min. The bromination reaction was continued for 2 h at room temperature, and water was poured to precipitate brominated PSF (Br-PSF). Then, Br-PSF was reprecipitated twice using n-hexane as a non-solvent to remove the unreacted bromine.

Cyanation of Br-PSF

Br-PSF dissolved in *N,N'*-dimethylformamide (DMF) was reacted with CuCN at 160°C for 6 h with refluxing DMF under a nitrogen atmosphere. The formed cyanated PSF (CN-PSF) was precipitated by 15 wt% ammonium hydroxide, and washed with 15 wt% ammonium hydroxide several times until the cobalt blue colour disappeared, and then with distilled water until the pH of the filtered water became 7. Then, CN-PSF was reprecipitated by n-hexane and dried in a vacuum oven for 12 h at 120°C.

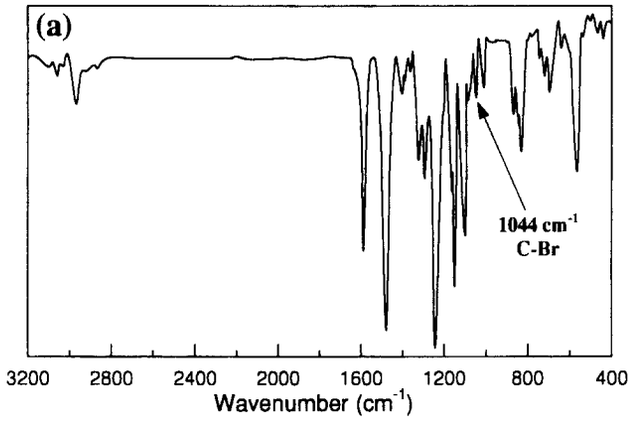

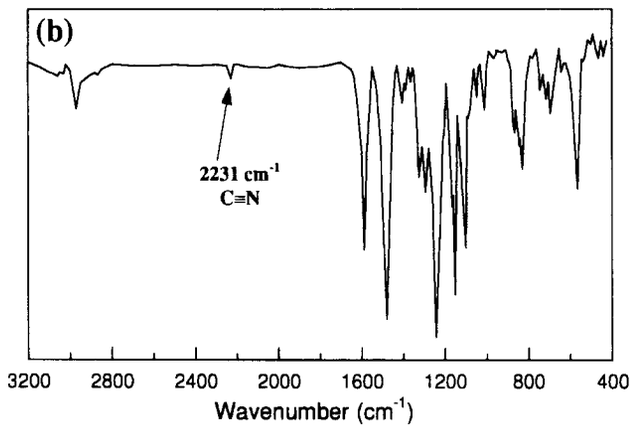

Figure 3 *FT* i.r. spectra of the modified polysulfone: (a) Br(5.5)-PSF; (b) CN(1.2)-PSF

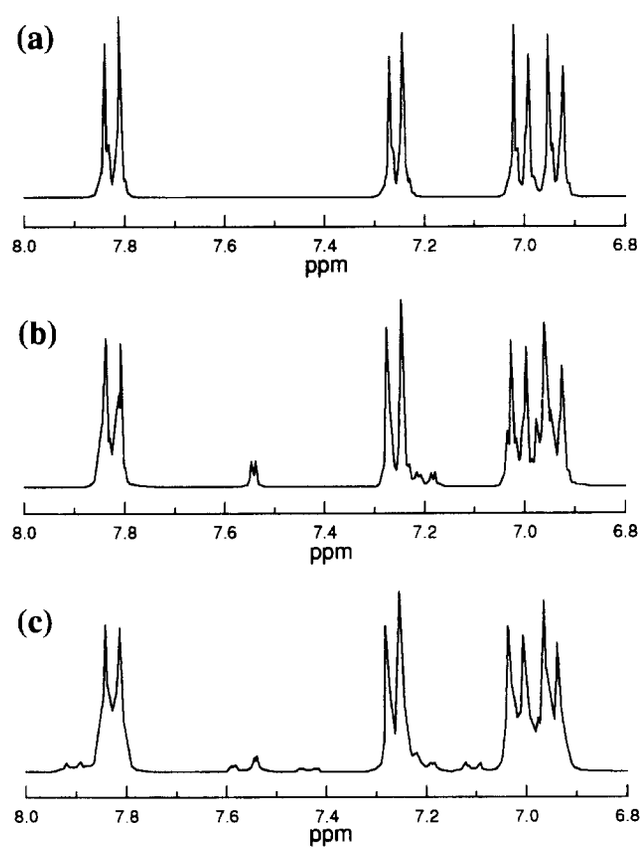

Figure 4 ^{1}H n.m.r. spectra (300 MHz) of PSs: (a) neat PSF, (b) Br(5.5)-PSF and (c) CN(1.2)-PSF

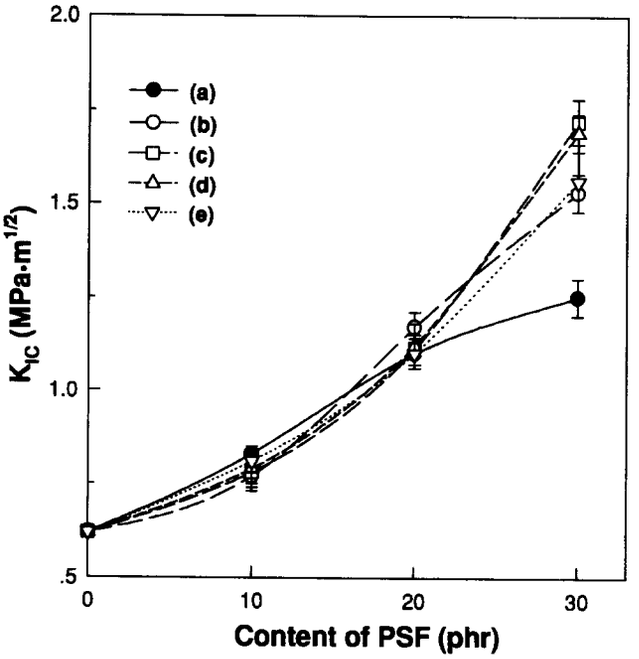

Figure 5 Fracture toughness *versus* PS content: (a) neat PSF, (b) CN(0.6)-PSF, (c) CN(1.2)-PSF, (d) CN(1.6)-PSF and (e) CN(2.1)-PSF

Sample preparation

PSF was dissolved in methylene chloride and mixed with BADCy at room temperature. The solution was heated in an oil bath for 1 h at 120–130°C to drive off most of the methylene chloride, and then the residual solvent and air bubbles were removed under vacuum for 30 min above 130°C. The blended resin was then poured into a Teflon-coated aluminium plate mould, and cured at 200°C for 4 h and at 250°C for 4 h in the oven to obtain fully cured samples. Pellets of neat PSF were also compression moulded at 270°C under 5 MPa.

Mechanical properties

Fracture toughness, K_{IC}, was measured by the notched three-point bending test with a crosshead speed of 1.0 mm min^{-1} according to ASTM E399. Fracture toughness was calculated using the following equation:

$$K_{IC} = \frac{P_C S}{BW^{3/2}} f\left(\frac{A}{W}\right) \quad (1)$$

where

$$f\left(\frac{A}{W}\right) = 3\left(\frac{A}{W}\right)^{1/2} \times \frac{[1.99 - (A/W)(1 - A/W)(2.15 - 3.93A/W + 2.7A^2/W^2)]}{[2(1 + 2A/W)(1 - A/W)^{3/2}]}$$

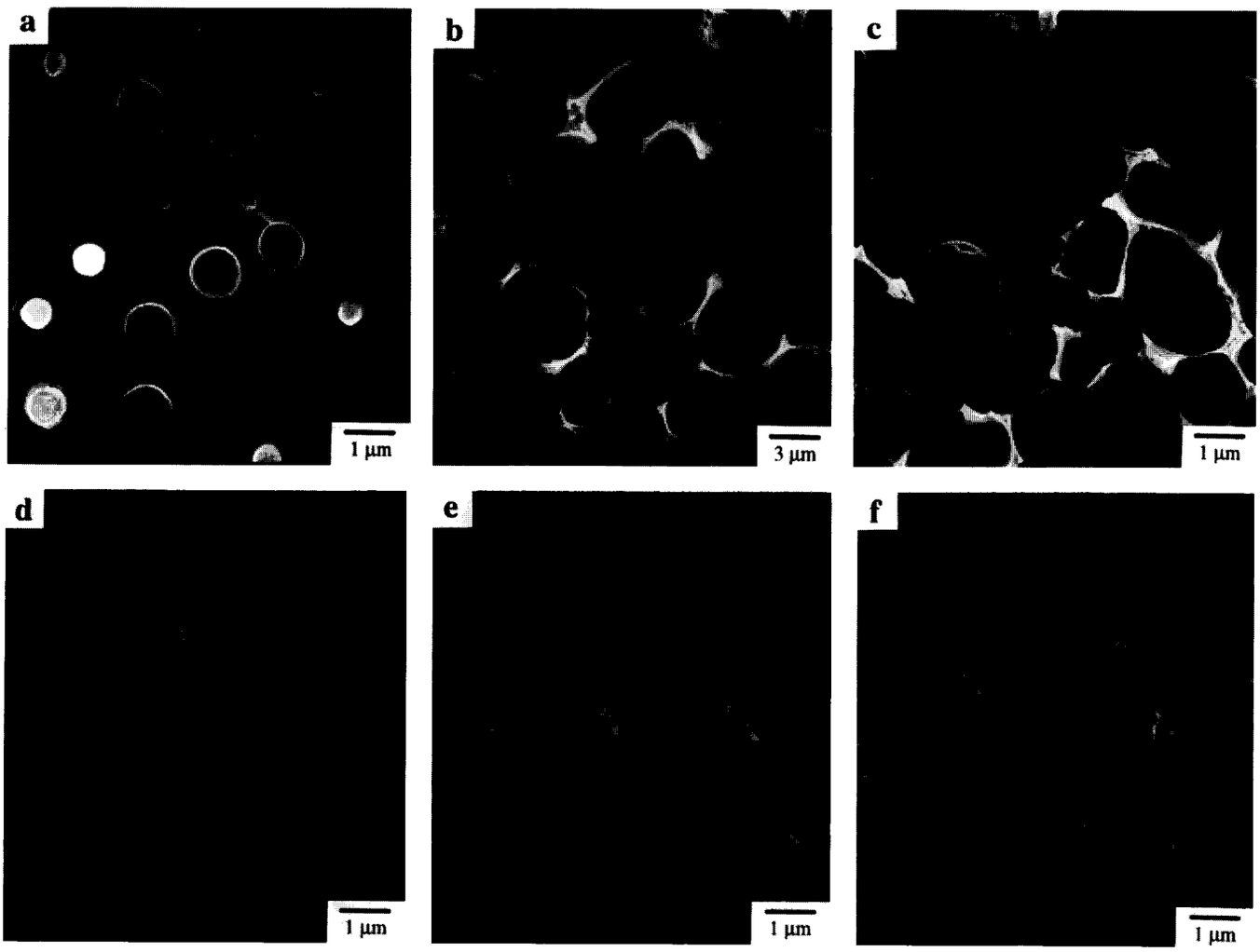

Figure 6 Scanning electron micrographs of the fracture surfaces of BADCy/neat PSF blends ((a) 10 phr, (b) 20 phr and (c) 30 phr of neat PSF) and BADCy/CN(0.6)-PSF blends ((d) 10 phr, (e) 20 phr and (f) 30 phr of CN-PSF)

and P_C is the load at crack initiation, B is the thickness of the specimen (3 mm), S is the span width (24 mm), W is the width of the specimen (6 mm) and A is the crack length (3 ± 0.3 mm). Central V-notches were machined in the bars and extended by pressing a fresh razor blade into the tip of the notch to give a crack length of 3 ± 0.3 mm. Flexural properties were measured by the three-point bending test with a crosshead speed of 1.28 mm min^{-1} according to ASTM D790. The dimensions of the specimens were $60 \times 12 \times 3$ mm with a span of 48 mm.

Microscopy

Fracture surfaces of the modified BADCy resins were examined by scanning electron microscopy. To examine the toughening mechanisms, the double-notched four-point bending test was employed. The mature process zone at the crack tip of the double-notched four-point bending (DN-4PB) specimen was examined by transmission optical microscopy. *Figure 2* shows the geometry of the DN-4PB specimen. There are two nearly identical sharp cracks cut into the same edge of the specimen with a fresh razor blade. The ratio between the crack spacing and the crack length must be greater than 0.75 in order to eliminate the interaction between the two cracks. The specimens were tested at a crosshead speed of 1.0 mm min^{-1}. Loading the specimen, one crack will propagate but the other will not because the cracks cannot be identical. Therefore the stationary crack has the mature process zone at the crack tip. Thin sections were taken in the midplane (plane strain region) near the stationary crack of the fractured surface and parallel to the fracture direction. A petrographic polishing technique was employed to obtain thin sections of about 100 μm for transmission optical microscopy.

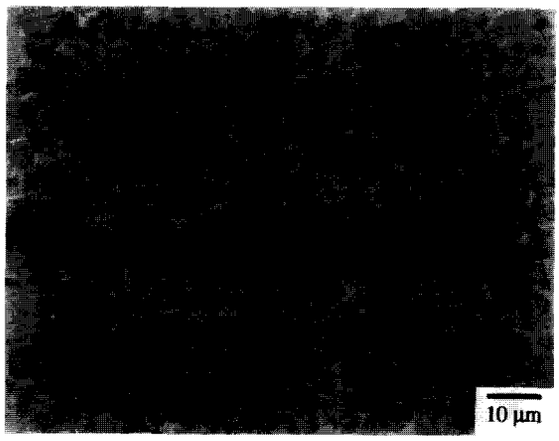

Figure 7 Crack propagation of the BADCy particle structure of BADCy/PSF blend with 20 phr of PSF content

RESULTS AND DISCUSSION

Modification of PSF

Figure 3 is the *FT*i.r. spectra of Br(5.5)-PSF and CN(1.2)-PSF showing the characteristic peaks of aromatic C–Br and C≡N at 1044 and 2231 cm^{-1}, respectively. In this paper, the average number of bromo and cyano groups per PSF chain are indicated in the parentheses after 'Br' and 'CN'. For example, Br(5.5)-PSF and CN(1.2)-PSF represent 5.5 bromo and 1.2 cyano groups, respectively, introduced per PSF chain. The average number of bromo and cyano groups per PSF chain was calculated from the elementary analysis data, and the measured number-average

Table 1 Flexural properties of PSF-modified BADCy resins

Specimens[a]	Flexural strength (MPa)	Flexural strain (%)	Flexural modulus (MPa)
Neat BADCy	195.9 ± 3.7	7.4 ± 0.3	3112 ± 51
Neat PSF	127.6 ± 1.1	6.5 ± 0.1	2640 ± 38
BADCy/neat PSF (10 phr)	185.4 ± 7.3	6.9 ± 0.6	3107 ± 64
BADCy/neat PSF (20 phr)	183.8 ± 9.0	4.5 ± 0.2	3200 ± 114
BADCy/neat PSF (30 phr)	130.8 ± 2.9	4.5 ± 0.2	3106 ± 51
BADCy/CN(0.2)-PSF (30 phr)	159.8 ± 5.4	5.9 ± 0.4	3177 ± 88
BADCy/CN(0.6)-PSF (10 phr)	166.5 ± 7.5	7.3 ± 1.2	2789 ± 61
BADCy/CN(0.6)-PSF (20 phr)	149.6 ± 12.5	5.8 ± 0.8	2844 ± 69
BADCy/CN(0.6)-PSF (30 phr)	141.3 ± 3.6	5.0 ± 0.2	2887 ± 61
BADCy/CN(1.2)-PSF (10 phr)	170.3 ± 5.1	7.0 ± 0.5	2925 ± 66
BADCy/CN(1.2)-PSF (20 phr)	154.2 ± 7.3	6.6 ± 1.3	2797 ± 153
BADCy/CN(1.2)-PSF (30 phr)	158.0 ± 9.8	7.4 ± 1.7	2805 ± 132
BADCy/CN(1.6)-PSF (10 phr)	142.9 ± 5.4	5.2 ± 1.5	3079 ± 188
BADCy/CN(1.6)-PSF (20 phr)	169.7 ± 14.9	6.7 ± 0.6	2967 ± 147
BADCy/CN(1.6)-PSF (30 phr)	165.1 ± 8.3	7.1 ± 1.2	2911 ± 86
BADCy/CN(2.1)-PSF (10 phr)	182.3 ± 14.3	8.3 ± 1.6	2806 ± 85
BADCy/CN(2.1)-PSF (20 phr)	161.4 ± 14.0	7.5 ± 1.2	2659 ± 153
BADCy/CN(2.1)-PSF (30 phr)	127.9 ± 22.2	4.8 ± 0.9	2860 ± 128
BADCy/CN(2.6)-PSF (30 phr)	149.4 ± 6.7	5.9 ± 0.7	2998 ± 71

[a] In the notation for BADCy/PSF blends, for example, BADCy/CN(0.2)-PSF (30 phr) indicates that the average number of CN groups substituted in the PSF backbone per PSF chain is 0.2 and the weight ratio of BADCy/PSF blend is 100/30

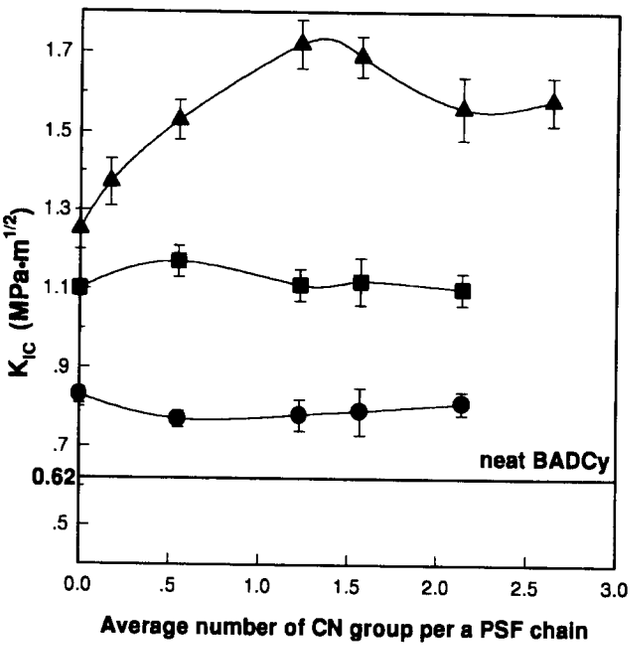

Figure 8 Fracture toughness versus the average number of CN groups per PSF chain: 10 phr of CN-PSF (●), 20 phr of CN-PSF (■) and 30 phr of CN-PSF (▲)

molecular weight of PSF using gel permeation chromatography and low-angle laser light scattering. In the spectrum of CN(1.2)-PSF, aromatic C–Br peaks were still seen. This indicates that the bromo groups were not substituted entirely by cyano groups by the cyanation reactions. *Figure 4* shows ^{1}H n.m.r. spectra of neat PSF, Br(5.5)-PSF and CN(1.2)-PSF. In the spectrum of neat PSF, four doublet peaks from the benzene ring are observed, indicating four different groups of hydrogen peaks. The formation of new peaks and a shift in the peaks are observed on introducing the bromo group into PSF, and further peaks and a shift in the peaks are seen on replacing bromo groups with cyano groups. Since it was impossible to quantify the bromo and cyano group peaks in the modified PSF from the ^{1}H n.m.r. study, elementary analysis was used to ascertain the number of bromo and cyano groups per PSF chain.

Fracture toughness and morphologies

The fracture toughness of BADCy was improved by incorporating PSF as a toughening agent. The fracture toughness of BADCy/PSF blends increased with increasing PSF content (*Figure 5*). Up to 20 parts per hundred of resin (phr) of PSF content, the improvement in the fracture toughness of BADCy/CN-PSF blends was the

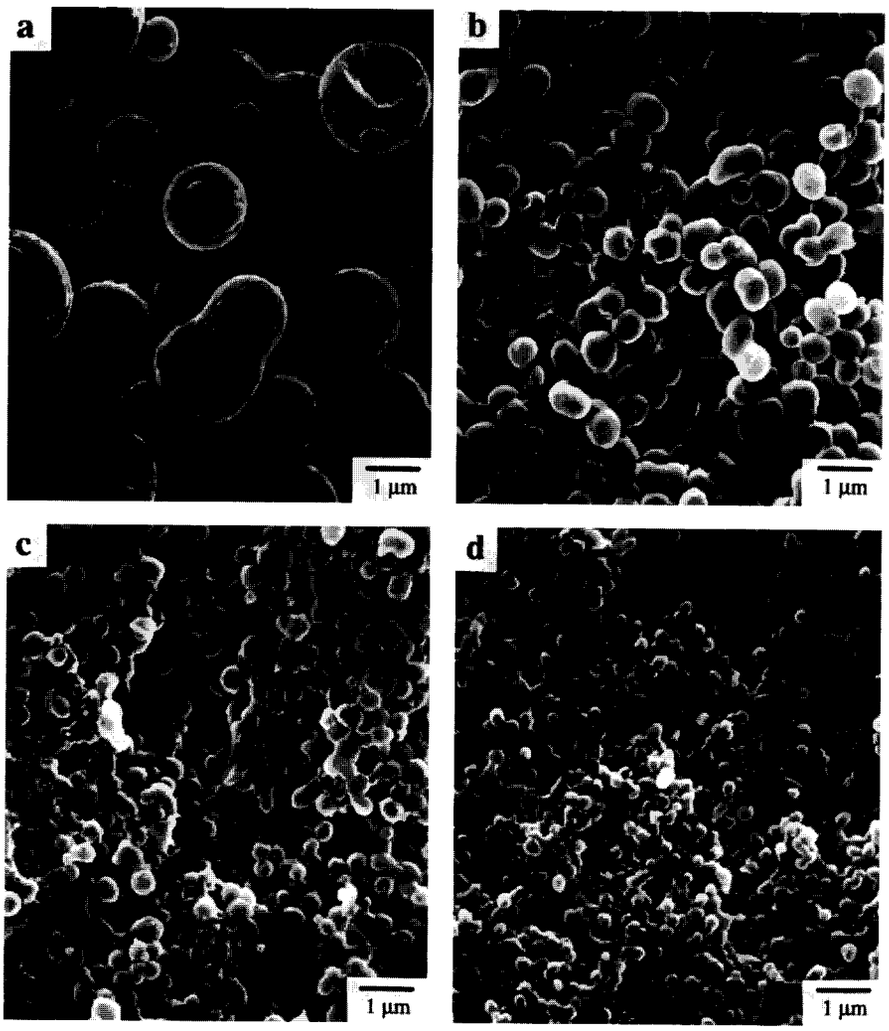

Figure 9 Scanning electron micrographs of the fracture surfaces of the BADCy/neat PSF blend with 30 phr of neat PSF content and BADCy/CN-PSF blends with 30 phr of CN-PSF content after etching PSF with methylene chloride: (a) BADCy/neat PSF (30 phr), (b) BADCy/CN(0.2)-PSF (30 phr), (c) BADCy/CN(0.6)-PSF (30 phr), (d) BADCy/CN(1.2)-PSF (30 phr), (e) BADCy/CN(1.6)-PSF (30 phr), (f) BADCy/CN(2.1)-PSF (30 phr) and (g) BADCy/CN(2.6)-PSF (30 phr)

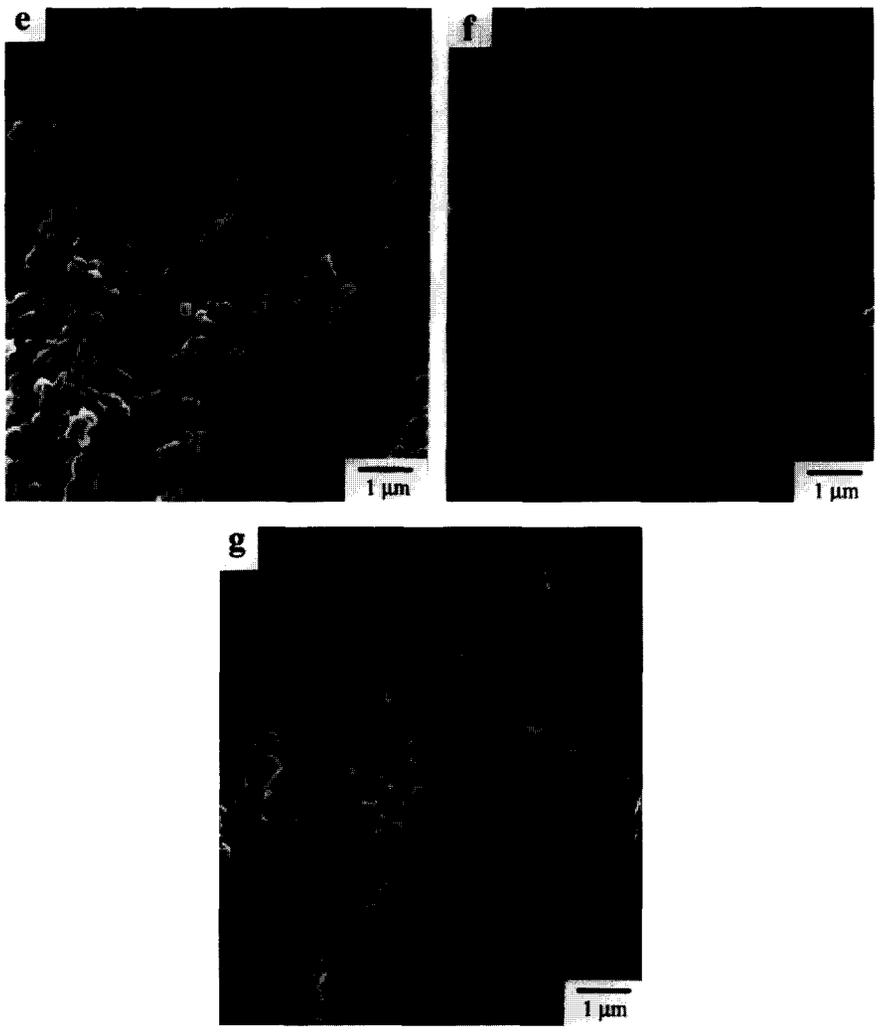

Figure 9 (Continued)

same as that of BADCy/neat PSF blends. However, for 30 phr of PSF content, the fracture toughness of BADCy/CN-PSF blends was much higher than that of BADCy/neat PSF blends. *Figure 6* shows the morphology of BADCy/PSF blends. With BADCy/neat PSF blends, a 0.5–1.0 μm spherical PSF particle structure is formed for 10 phr of PSF content, and BADCy particle structures are formed for 20 and 30 phr of PSF content. The size of BADCy particles is 4–8 and 1–2 μm for 20 and 30 phr of PSF content, respectively. In the fracture surfaces of BADCy particle structures, poor adhesion between the PSF matrix and BADCy domain was observed. In contrast, with BADCy/CN(0.6)-PSF blends, a smaller size of PSF particles (0.2–0.3 μm) for 10 phr of CN(0.6)-PSF content, a mixture of PSF particle structure and BADCy particle structure for 20 phr of CN(0.6)-PSF content, and BADCy particle structure with a smaller size of BADCy particles (0.3–0.4 μm) for 30 phr of CN(0.6)-PSF content, are formed. The above difference in the morphology arises from the chemical reactions between the CN groups of CN-PSF and the cyanate groups of BADCy. A smaller domain size of particles in the PSF particle structure and BADCy particle structure, and better adhesion between the matrix and domain, seem to be caused by the chemical reactions. The crack propagates through the BADCy matrix for the PSF particle structure, and along the PSF matrix and/or the interface between the PSF matrix and the BADCy particles for the BADCy particle structure (*Figure 7*). Therefore, the adhesion strength between the PSF matrix and the BADCy particles determines the fracture toughness of BADCy/PSF blends in the BADCy particle structure. Since CN-PSF-modified BADCy resin has better interfacial adhesion than neat PSF-modified BADCy resin, the fracture toughness of CN-PSF-modified BADCy resin was higher than that of neat PSF-modified BADCy resins with 30 phr of PSF content. With 20 phr of PSF content, the fracture toughness of the BADCy/CN-PSF blend was the same as that of the BADCy/neat PSF blend because the morphology of the BADCy/CN-PSF blend is a mixture of the PSF particle structure and the BADCy particle structure instead of solely the BADCy particle structure shown by the BADCy/neat PSF blend: the fracture toughness of the BADCy particle structure is higher than that of the PSF particle structure. Flexural strength, flexural strain and flexural modulus of PSF modified BADCy resins decreased compared to the BADCy resin because of the lower flexural properties of PSF compared to BADCy resins, as shown in *Table 1*.

Figure 8 shows the fracture toughness of BADCy/CN-PSF blends depending on the average number of CN groups per PSF chain. The fracture toughness of BADCy resin was 0.62 MPa $m^{1/2}$, as indicated by the solid line.

Table 2 Morphology and particle size of BADCy resins versus the average number of CN groups per PSF chain

	No. of CN groups per PSF chain						
	0.0	0.2	0.6	1.2	1.6	2.1	2.6
Morphology	BADCy particle structure	BADCy particle structure	BADCy particle structure	BADCy particle structure	BADCy particle structure	Co-continuous structure	Co-continuous structure
Particle size of BADCy resins (μm)	1.96 ± 0.62	0.65 ± 0.11	0.40 ± 0.08	0.25 ± 0.05	0.25 ± 0.08	—	—

The effects of the number of CN groups per PSF chain on the fracture toughness were not seen with 10 and 20 phr of CN-PSF content. However, for 30 phr of CN-PSF content, maximum fracture toughness was obtained with 1.2 CN groups per PSF chain. *Figure 9* shows scanning electron micrographs of the fractured surfaces of the BADCy/neat PSF blend with 30 phr of neat PSF content and BADCy/CN-PSF blends with 30 phr of CN-PSF content after etching PSF with methylene chloride. Spherical particles of BADCy resins are clearly seen after etching the PSF matrix from the BADCy/neat PSF blend (*Figure 9a*). The particle size of BADCy resin became smaller on introducing CN groups to the PSF, and decreased further with increasing numbers of CN groups per PSF chain (*Table 2*). Therefore, the fracture toughness increased with the increase in CN group per PSF chain up to 1.6. With 1.6 CN groups per PSF chain, the BADCy resin particle started to coalesce and form a connected structure. With more than 2.1 CN groups per PSF chain, the continuous phase of BADCy resin was seen: the co-continuous structure formed. The decrease in fracture toughness with more than 1.6 CN groups per PSF chain can be explained by the change of morphology from the BADCy particle structure to the co-continuous structure: the BADCy particle structure absorbs more energy than the co-continuous structure. *Figure 10* shows the fracture toughness of BADCy/neat PSF/CN(2.6)-PSF blends with 30 phr of total PSF content depending on the mass ratio of CN(2.6)-PSF/neat PSF. Maximum fracture toughness was obtained when the mass ratio of CN(2.6)-PSF/neat PSF was 60/40. If the x axis is converted to the average number of CN groups per PSF chain for the total PSF content calculated from the mass ratio of CN(2.6)-PSF/neat PSF, *Figure 10* is very similar to the curve of BADCy/CN-PSF blends with 30 phr of CN-PSF content shown in *Figure 8*. This confirms that the fracture toughness of PSF-modified BADCy resins depends on the average number of CN groups in the PSF, which determines the morphology of PSF-modified BADCy resins. *Figure 11* shows scanning electron micrographs of BADCy/neat PSF/CN(2.6)-PSF blends with 30 phr of total PSF content. Similar to *Figure 9*, by increasing the mass ratio of CN(2.6)-PSF/neat PSF, the particle size of BADCy resins decreased, and the co-continuous structure was obtained with a CN(2.6)-PSF/neat PSF ratio above 0.8. It is also very clear that the adhesion between the PSF matrix and the BADCy particles is poor without CN groups in the PSF, and that the adhesion improves with an increase in the number of CN groups in the PSF. *Figure 12* shows transmission optical micrographs of thin sections taken mid-plane and near the crack tip of DN-4PB samples of BADCy/PSF blends with 30 phr of PSF content. In the BADCy/neat PSF blend, limited

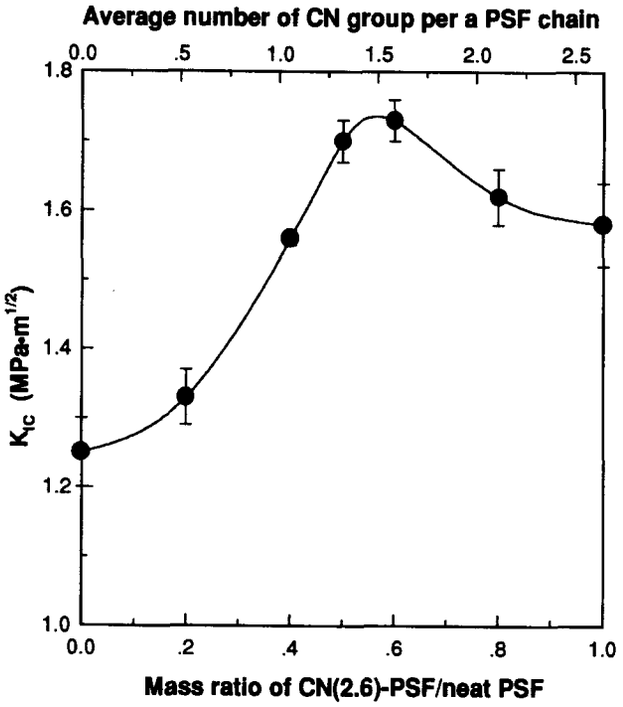

Figure 10 Fracture toughness of BADCy/neat PSF/CN(2.6)-PSF blends *versus* the mass ratio of CN(2.6)-PSF/neat PSF. The total amount of PSF is 30 phr

deformation near the crack line was observed (*Figure 12a*). In contrast in the BADCy/CN(1.2)-PSF blend, a large deformation zone near the crack tip was observed (*Figure 12b*). It appears that the dense black lines are due to the shear deformation of PSF matrix. We believe that the larger deformation zone originates from the increase of interfacial adhesion between the PSF matrix and the BADCy particles, which is related to the increase in fracture toughness.

CONCLUSIONS

The fracture toughness of BADCy/PSF blends increased with increasing PSF content. Up to 20 phr of PSF content, the effects of CN groups in PSF on the fracture toughness of BADCy/PSF blends were not seen. However, for 30 phr of PSF content, the fracture toughness of BADCy/CN-PSF blends was much higher than that of BADCy/neat PSF blends. There was also an optimum CN group content for maximizing the fracture toughness of BADCy/CN-PSF blends. The highest K_{IC}, 1.72 MPa $m^{1/2}$, was obtained with 1.2 cyano groups per PSF chain for 30 phr of PSF content. With BADCy/neat PSF blends, a 0.5–1.0 μm spherical PSF particle structure was

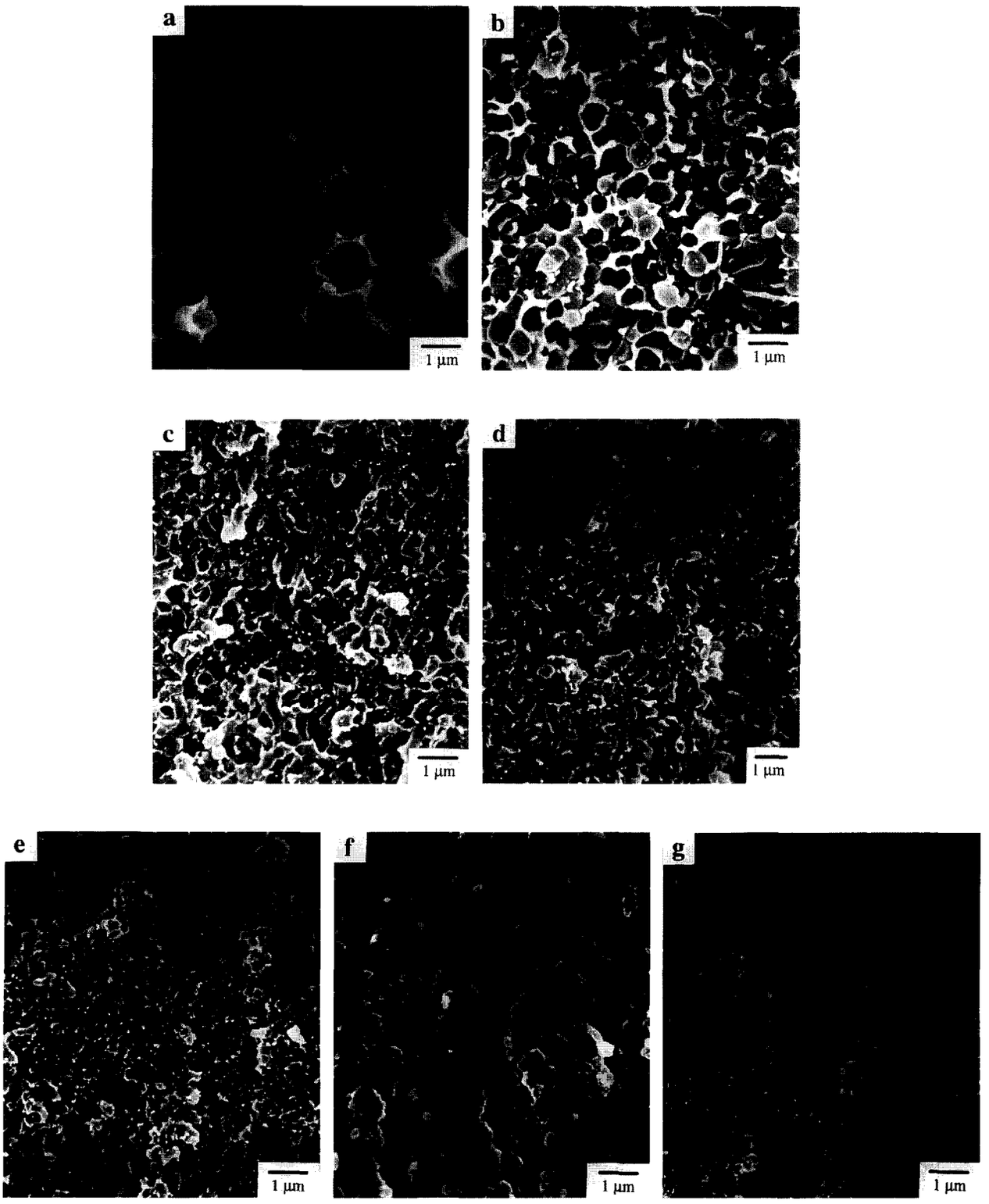

Figure 11 Scanning electron micrographs of the fracture surfaces of the blend of BADCy/neat PSF/CN(2.6)-PSF: CN(2.6)-PSF/neat PSF is varied as (a) 0/100, (b) 20/80, (c) 40/60, (d) 50/50, (e) 60/40, (f) 80/20 and (g) 100/0

formed for 10 phr of PSF content, and BADCy particle structures were formed for 20 and 30 phr of PSF content. By introducing CN groups into the PSF backbone, a smaller size of PSF particles with 10 phr of CN-PSF content, a mixture of PSF particle structure and BADCy particle structure with 20 phr of CN-PSF content, and BADCy particle structure with a smaller size of BADCy particles with 30 phr of CN-PSF content were formed, owing to the chemical reactions between the CN groups of CN-PSF and the cyanate groups of BADCy. The increase in interfacial adhesion between the PSF matrix and the BADCy particles causes an increase in fracture toughness, and the damage zone originated from ductile yielding of PSF.

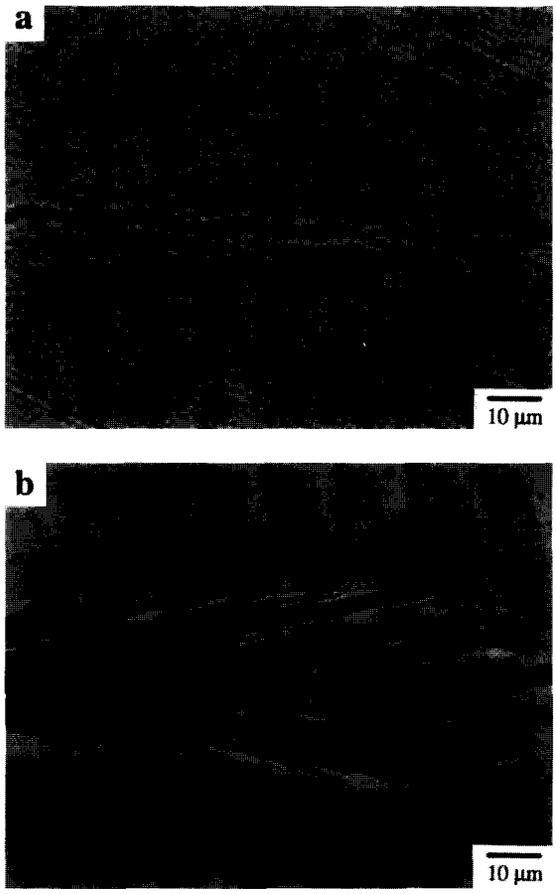

Figure 12 Transmission optical micrographs of thin sections taken mid-plane and near the crack tip of DN-4PB samples of BADCy/PSF blends with 30 phr of PSF content: (a) BADCy/neat PSF and (b) BADCy/CN(1.2)-PSF

ACKNOWLEDGEMENT

This work was supported by a research grant of New Materials from the Ministry of Education.

REFERENCES

1 Novak, H. L. and Comer, D. A. *Adhesive Age* 1990, Feb., 28
2 McGonnell, V. P. *Adv. Composites* 1972, May/June, 28
3 Shimp, D. *Polym. Mater. Sci. Eng.* 1994, **71**, 623
4 Graver, R. B. *Polym. Prepr.* 1990, **27**, 491
5 Simon, S. L. and Gillham, J. K. *J. Appl. Polym. Sci.* 1993, **47**, 461
6 Osei-Owusu, A. and Martin, G. C. *Polym. Eng. Sci.* 1992, **32**, 535
7 Bauer, M., Bauer, J. and Jährig, S. *Makromol. Chem., Macromol. Symp.* 1991, **45**, 97
8 Papathomas, K. I. and Wang, D. W. *J. Appl. Polym. Sci.* 1992, **44**, 1267
9 Pearson, R. A. and Yee, A. F. *J. Mater. Sci.* 1989, **24**, 2571
10 Kim, D. S., Cho, K., An, J. H. and Park, C. E. *J. Mater. Sci. Lett.* 1992, **11**, 1197
11 Kim, D. S., Cho, K., An, J. H. and Park, C. E. *J. Mater. Sci.* 1994, **29**, 1854
12 Kim, D. S., Cho, K., Kim, J. K. and Park, C. E. *Polym. Sci. Eng.* 1996, **36**, 755
13 Cho, J. B., Hwang, J. W., Cho, K., An, J. H. and Park, C. E. *Polymer* 1993, **34**, 4832
14 Hourston, D. J. and Lane, J. M. *Polymer* 1992, **33**, 1379
15 Bucknall, C. B. and Gilbert, A. H. *Polymer* 1989, **30**, 213
16 Yamanaka, K. and Inoue, T. *Polymer* 1989, **30**, 662
17 Akay, M. and Cracknell, J. G. *J. Appl. Polym. Sci.* 1994, **52**, 663
18 Bennett, G. S., Farris, R. J. and Thompson, S. A. *Polymer* 1991, **32**, 1633
19 Srinivasan, S. A., Lyle, G. D. and McGrath, J. E. 18th International SAMPE Symposium, 10–13 May 1993, p. 28
20 Srinivasan, S. A., Joardar, S. S., Priddy, D. B., Ward, T. C. and McGrath, J. E. *Polym. Mater. Sci. Eng.* 1994, **70**, 93
21 Iijima, T., Suzuki, N., Fukuda, W. and Tomoi, M. *Eur. Polym. J.* 1995, **31**, 775
22 Kim, B. S., Chiba, T. and Inoue, T. *Polymer* 1995, **36**, 43
23 Hedrick, J. L., Yilgor, I., Jurek, M., Hedrick, J. C., Wilkes, G. L. and McGrath, J. E. *Polymer* 1991, **32**, 2020
24 Kubotera, K. and Yee, A. F. ANTEC, 3–7 May 1992, p. 2610